

DOI: 10.1070/QEL16134

Experimental and theoretical study of the heating dynamics of carbon-containing optothermal fibre converters for laser surgery

A.V. Belikov, A.V. Skrypnik, V.Yu. Kurnyshev, K.V. Shatilova

Abstract. **We have studied carbon-containing optothermal fibre converters (COTFCs) that are located on the distal end of a quartz–quartz optical fibre for delivering laser radiation in medical laser surgery systems and differ in the thickness and structure of the layer of a material converting laser radiation into heat. The heating dynamics of 'thin-film' and '3D' converters have been investigated at average incident 980-nm semiconductor laser beam powers of 0.3, 1.0 and 4.0 W, with the converters placed freely in air. The results demonstrate that, before the instant of disintegration, the efficiency of laser heating of the converter surface can reach 3000 °C W^{-1} for thin-film converters, 1000 °C W^{-1} for spherical 3D converters and 55 °C W^{-1} for planar 3D converters. The thin-film converter breaks down at an average laser beam power as low as 0.30 ± 0.05 W, which is accompanied by a considerable reduction in heating efficiency and is caused by the disintegration of the carbon film on its surface. The spherical 3D converter breaks down at an average power of 4.0 ± 0.1 W, as a result of the disintegration of the carbon film on its surface and partial melting of a modified layer containing microbubbles. The carbon film on the surface of the planar 3D converter also disintegrates at an average power of 4.0 ± 0.1 W, but the structure of the modified layer remains unchanged. We have constructed structural and optophysical models of the converters by simulating light absorption in carbon films on the surface of the COTFC and inside the microbubbles present in the modified layer of the converters. The proposed models of the COTFCs have been shown to adequately describe real converters.**

Keywords: *laser radiation, converter, quartz glass, carbon, fibre, efficiency, heating.*

1. Introduction

Laser radiation is widely used for processing various materials, in particular for excising biological tissues in medicine [1, 2]. In most laser surgical treatments, excision efficiency is higher at a larger absorption coefficient of the biological tissue [3]. Reaching biological tissue, laser radiation converts into heat, which leads to coagulation, vaporisation, carbonisation and excision of the biological tissue. CO_2 and erbium lasers are commonly thought to be the most efficient [1–5]: the absorption coefficient of soft biological tissues for their radiation is determined by the absorption in water. In particular, the absorption coefficient of water at the CO_2 laser wavelength (λ = 10.6 μm) is 825 cm^{-1} [6] and that at the Er:YAG laser wavelength (λ = 2.94 μm) is 12 200 cm^{-1} [6]. In recent years, laser surgery widely employed semiconductor lasers [1, 7–12] emitting in the near-IR spectral region at wavelengths λ = 0.81–0.98 μm. The output of these lasers is very weakly absorbed by soft biological tissues. The absorption coefficient of water at λ = 0.98 μm is known to be 0.5 cm^{-1} [13], the absorption coefficient of the mucous membrane in the range λ = 950–1000 nm is 0.4 cm^{-1} [14, 15], that of skin is 0.2–2.0 cm^{-1} [15, 16], and that of muscular tissue is 0.46–0.51 cm^{-1} [16].

Because of this, laser radiation energy is converted into heating of tissue with extremely low efficiency. As a result, biological tissues are excised with low efficiency, and there is a large damage (coagulation, denaturation or necrosis) zone [5, 17–19].

To improve the conversion efficiency from laser radiation to heat in contact laser surgery, a specialised converter is placed at the distal end of the fibre that delivers laser radiation to biological tissue. Soft biological tissue is then destroyed primarily as a result of contact with the converter, heated to high temperatures (up to 900 °C [20]). Unfortunately, there is still no generally accepted name (term) for such a type of converter, possibly because there is no sufficient knowledge of its nature and because there is a diversity of converter designs and functions. In a number of publications, it was referred to as 'an optothermal fibre converter' (OTFC) [14, 20–24]. In others, it was termed 'a blackened tip' [21, 25–28], 'hot tip' [29–34] or 'pre-initiated tip' [35]. The term 'hot tip' does not specify that the converter is placed at the fibre end, nor does it mention the converter material or how the laser energy is converted. It only informs that the converter is 'hot'. Note that the hot tip may have the form of a carbon layer on the fibre end face [29], or a metallic layer on optical fibre [30, 33] or merely a probe tip of an electrocoagulator [34], which has nothing in common with laser surgery facilities.

The term 'blackened tip' is used to denote a carbon-coated quartz fibre tip [25, 26, 28]. The carbon coating can be produced by exposing various materials, such as wood [25, 26, 28], biological tissue [21, 23, 31] or cork [23]. As pointed out by Skrypnik [20] and Van den Bos et al. [32], a blackened tip converts optical energy into thermal one. Such a converter can be used for both thermal and acoustic processing, i.e. it is capable of converting optical radiation into both heat and an acoustic wave, which have fundamentally different effects of

A.V. Belikov, A.V. Skrypnik, K.V. Shatilova St. Petersburg National Research University of Information Technologies, Mechanics and Optics, Kronverkskii prosp. 49, 197101 St. Petersburg, Russia; e-mail: meddv@grv.ifmo.ru, alesch_skrypnik@mail.ru, kshatilova@mail.ru;
V.Yu. Kurnyshev JSC Precision Systems and Instruments Research and Production Corp. (St. Petersburg Branch), Vasil'evskii Ostrov, Vtoraya liniya 5, 199034 St. Petersburg, Russia;
e-mail: vadimkurnyshev@gmail.com

Received 13 May 2016
Kvantovaya Elektronika **46** (6) 534–542 (2016)
Translated by O.M. Tsarev

biological systems [25–28, 36]. These data lead us to conclude that different groups use the term 'blackened tip' to denote converters with different functions.

Sivriver and Boutoussov [35] described a pre-initiated tip produced by depositing organic and inorganic pigments, metal powders or nonmetallic pigments onto the end of an optical fibre. The term used by them also gives no idea of where the converter is located or how the laser energy is converted. The term used in this report, OTFC, contains information about the location of the converter (fibre) and how the laser energy is converted (optothermal). With the main light conversion material (carbon) included in the converter's name, we obtain 'a carbon-containing optothermal fibre converter' (COTFC) instead of OTFC.

In a number of cases, medical lasers include temperature control systems of their optothermal converters, as well as automatic beam power correction systems [21]. Altshuler et al. [14, 22] described a system in which the OTFC temperature was maintained at a predetermined level during biological tissue processing. The higher the temperature of a converter, the more efficient it is in destroying (excising) soft biological tissue [37]. The maximum temperature to which a converter can be heated without damage and which can be maintained by its automatic control system is determined, among other factors, by the structure and properties of the converter itself, which in turn depend on the converter fabrication process. Optothermal converters can be produced by a variety of techniques. Unfortunately, there is very limited information about the structure of different types of OTFCs and the efficiency of heating them by laser radiation. Moreover, there are no data that would enable an adequate comparison of converters differing in structure and no relevant structural or optophysical models of converters.

In all the types of converters examined in this study, the light conversion layer contains carbon [29, 36, 38]. Converters of the first type are produced as described in Refs [25, 38, 39] and have the form of an amorphous carbon film [25, 38–40] ('thin-film' converters). Converters of the second type are produced as described in Refs [20, 36] and have the form of a carbon-coated modified layer consisting of amorphous carbon and quartz glass. The thickness of the layer may reach 100 μm or more ('3D' converter). This type can be divided into planar 3D and spherical 3D converters, depending on the shape and position of the modified layer. The planar 3D converters are similar in diameter to their optical fibre and their modified layer is typically located on the fibre end. The spherical 3D converters are almost hemispherical in shape, their diameter considerably exceeds the fibre diameter, and their modified layer is located on both the facet and lateral surface of the distal fibre end.

The structure of the 3D COTFCs was described in detail in a previous study [41], where optical microscope examination of converters and their polished sections showed that the carbon film of the COTFCs contained quartz glass, with microinclusions embedded in it. Colouring of polished sections of a 3D converter showed that the microinclusions had the form of hollow microbubbles, with a carbon film on their walls [41], and originated from the melting of quartz glass in air as a result of laser heating to temperatures above 1500 °C [42]. A characteristic microbubble diameter in the 3D COTFCs was determined to be 19.6 ± 0.9 μm [41].

The objectives of this study are to perform an experimental comparison of the efficiency of laser heating of the surface of thin-film and 3D converters in air; determine the average power of a 980-nm semiconductor laser at which heating efficiency remains constant for a long time; construct adequate structural models of thin-film, planar 3D and spherical 3D converters; model the laser heating of the converters; and compare the calculated converter temperature to experimental data.

2. Fabrication techniques and optical microscope examination of the COTFC structure

In this study, converters were produced using an Alta-ST semiconductor laser (Dental Photonics, Inc., USA). Its output radiation at a wavelength of 980 ± 10 nm was delivered through a quartz–quartz optical fibre [23]. The fibre core diameter was 400 ± 5 μm (Fig. 1) and the total fibre diameter was 440 ± 5 μm after stripping the polymer coating and 475 ± 10 μm with the coating. The average power at the fibre output was 25 W. The laser output had the form of a train of 400-μs pulses with a repetition rate of 2 kHz. The laser pulse train duration was 12.0 ± 0.1 s.

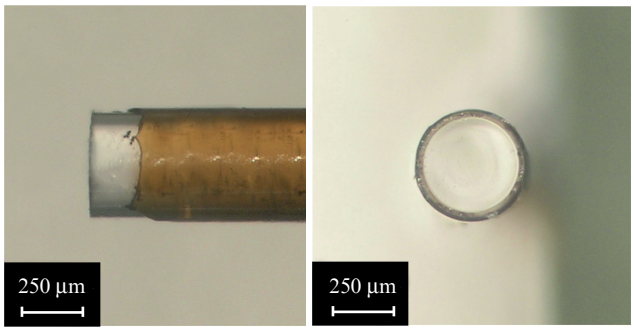

Figure 1. Appearance of the distal end of a quartz–quartz optical fibre.

The Alta-ST system has a unique built-in system for measuring the temperature of the distal fibre end. The converter is located at this end. The system measures the power of the thermal radiation resulting from the laser heating of the OTFC by laser radiation delivered to the converter through the optical fibre. The thermal radiation propagates from the converter through the same fibre but in a direction opposite to that of the laser radiation. At the fibre input, the thermal radiation is separated from the laser radiation by a spectrum splitter and detected by an FD10D IR detector (Thorlabs, USA). The detector signal is sent to an analog-to-digital converter (ADC) and then converted to the temperature using a calibration curve. Calibration is performed by comparing the amplitude of the IR detector signal at the ADC output to the temperature measured on the converter surface using a Fluke Ti400FT thermal imaging camera (Fluke, USA) in the range 300–800 °C and a Promin' pyrometer (Kamianets-Podilskyi Instrumentation Plant, Ukraine) in the range 800–2500 °C. The sensitivity limit of the system is ~390 °C because of the limited sensitivity of the IR detector and the intrinsic noise in the input channel. The ADC allows the temperature to be measured every 30 ms, with uncertainty within 5%. The measured converter temperature is displayed in real time in a window of the stLase-1.19 programme (Dental Photonics, Inc., USA) when the data are fed to a personal computer through a USB port.

A thin-film converter was fabricated by a procedure used in previous studies [25, 38, 39], where converters were produced on the distal end of a quartz glass fibre 300–400 μm in diameter [25, 38] by laser irradiation at 940 [38] or 970 nm [25], at output powers from 1 [38, 39] to 3 W [25] and an exposure time of 1 s [25] in air, with the fibre brought into contact with wood [25] or cork [38]. The converters were used in studies reported by Yusupov et al. [25], clinical practice [38] and commercially available laser surgery systems [39]. In this study, the distal fibre end face in the thin-film converter was in contact with the planar surface of a cork target. The converter was exposed to the semiconductor laser beam with an average power of 1.0 ± 0.1 W for 1.00 ± 0.01 s. As a result, the target was destroyed and the products deposited onto the surface of the distal fibre end to form a film (Figs 2a, 2b).

To produce a planar 3D converter, the distal fibre end was brought into contact with a planar surface of an activated carbon target and the converter was exposed to a semiconductor laser beam with a maximum average power of up to 12.5 ± 0.1 W for 0.50 ± 0.01 s. As a result, the target was destroyed and the products deposited onto the surface of the distal fibre end. After that, the distal fibre end was kept freely in air and the converter was exposed to two semiconductor laser pulses with a maximum average power of 8.0 ± 0.1 W of 1.00 ± 0.01 s duration, with a separation of 0.50 ± 0.01 s, to produce a modified layer (Figs 3a, 3b).

To produce a spherical 3D converter, the distal fibre end was brought into contact with a planar surface of an activated carbon target and the converter was exposed to a semiconductor laser beam with a maximum average power of up to 15.0 ± 0.1 W for 0.50 ± 0.01 s. As a result, the target was destroyed and the products deposited onto the surface of the distal fibre end. After that, the distal fibre end was kept freely in air and the converter was exposed to two semiconductor laser pulses with a maximum average power of 10.0 ± 0.1 W of 1.00 ± 0.01 s duration, with a separation of 0.50 ± 0.01 s, to produce a modified layer (Figs 4a, 4b).

It is worth noting that the presence of carbon in the film on the surface of all the converters under consideration was confirmed in several studies [12, 25, 29, 36, 38]. According to X-ray diffraction results [29, 36], the surface of a 3D converter produced under conditions similar to those described above, may contain a considerable amount of carbon (more than 88%).

To photograph the converters and determine their geometric dimensions, we used an AxioScope A1 microscope (Carl Zeiss GmbH, Germany) and the AxioVision rel.4.8.2 program (Carl Zeiss GmbH, Germany), which allows the size of an object placed in the field of view of the microscope to be determined with an accuracy of 1 μm. The average measured size, e.g. the diameter of each type of converter, was evaluated from ten independent measurements.

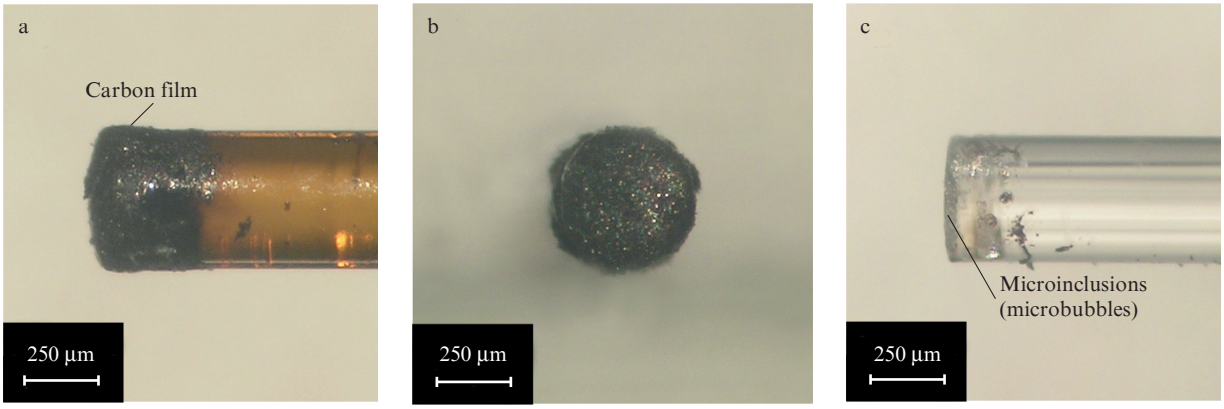

Figure 2. Appearance of a thin-film COTFC (a, b) before and (c) after exposure to the beam of a semiconductor laser operating at a wavelength of 980 nm and average power of 4 W.

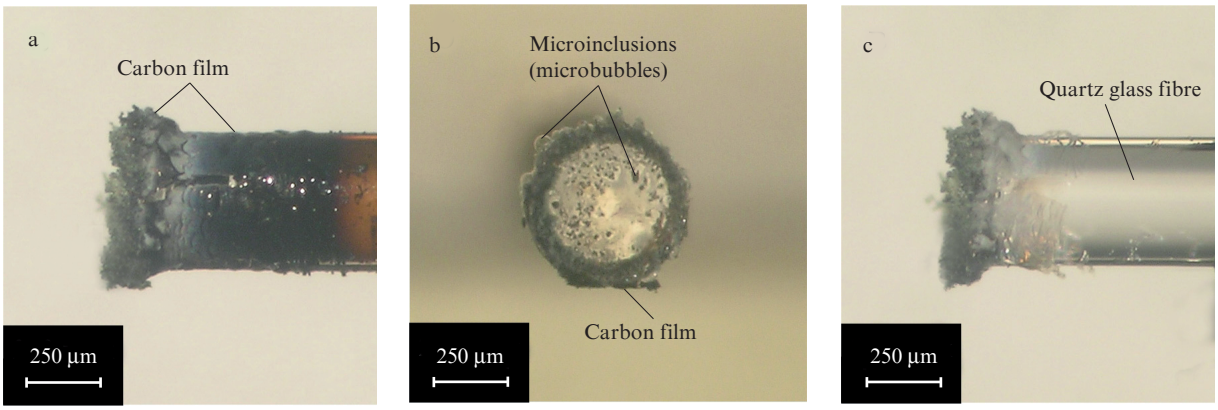

Figure 3. Appearance of a planar 3D COTFC (a, b) before and (c) after exposure to the beam of a semiconductor laser operating at a wavelength of 980 nm and average power of 4 W.

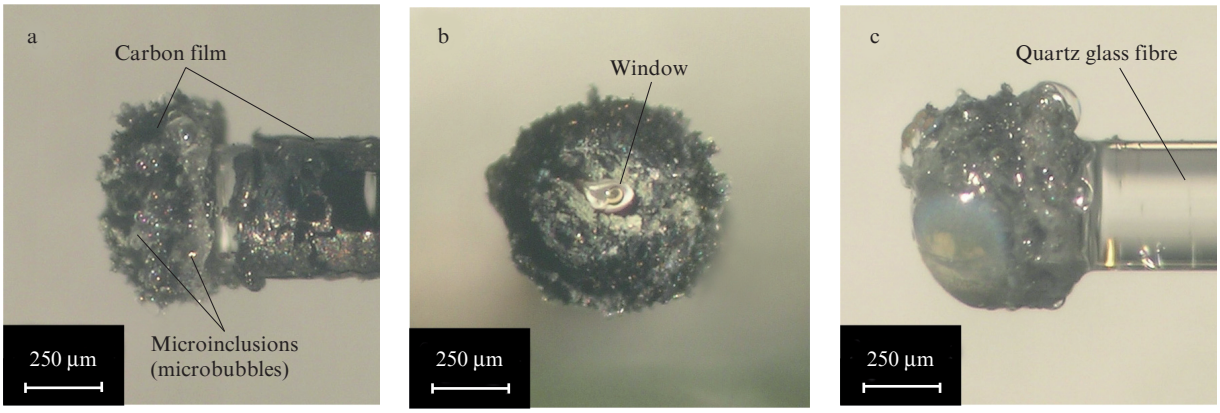

Figure 4. Appearance of a spherical 3D COTFC (a, b) before and (c) after exposure to the beam of a semiconductor laser operating at a wavelength of 980 nm and average power of 4 W.

The diameter of the thin-film converter was determined to be 500 ± 20 μm. The carbon film covered the end face and lateral surface of the converter. The thickness of the carbon film on the surface of the thin-film COTFC was up to 50 μm.

The diameter of the planar 3D COTFC was 550 ± 20 μm. The lateral surface of the COTFC had a carbon coating. Microinclusions were present on the lateral surface within about 150 μm from the end face, which means that the planar 3D converter was of the order of 150 μm in length. The end face of the converter had no carbon film.

The diameter of the spherical 3D COTFC was 680 ± 20 μm and its length was 340 ± 20 μm. The lateral surface and end face of the COTFC were covered with a carbon film. In its centre, on the longitudinal fibre axis, the COTFC had a transparent 'window' 150 ± 20 μm in diameter, which was surrounded by microinclusions.

3. Experimental study of the heating dynamics of the COTFC

To study the temperature dynamics of the converters at a varied average incident laser power, the COTFCs were placed freely in air and the semiconductor laser beam with an average output power of 0.30 ± 0.05, 1.0 ± 0.1 or 4.0 ± 0.1 W propagated through the optical fibre, which had a converter on its distal end. The COTFCs were exposed to the laser beam for 12.0 ± 0.1 s. The time variation of the converter temperature was monitored at 30-ms intervals. At each average laser power in our experiments, we studied the heating dynamics of ten converter samples of each of the types described above.

Figure 5 presents results of the most characteristic experiment. Since the measuring system was calibrated by determining the temperature in a point on the lateral converter surface facing the pyrometer (thermal imaging camera) and located of the order of 100 μm from the output end of the converter, Fig. 5 illustrates the heating dynamics of this region.

It is seen that the heating dynamics of the OTFCs depends on the type of converter and the average power of incident laser radiation. When exposed to laser radiation of constant power, the converters heat up to different temperatures, break down after different lengths of time and differ in shape. To compare these devices in our experimental study, we use a converter heating efficiency parameter. Since the fraction of laser radiation converted into thermal energy in the converters cannot be evaluated in experiments, the heating efficiency parameter has the characteristic dimensions of temperature divided by power. We believe that the comparison in question is correct because we used identical experimental conditions

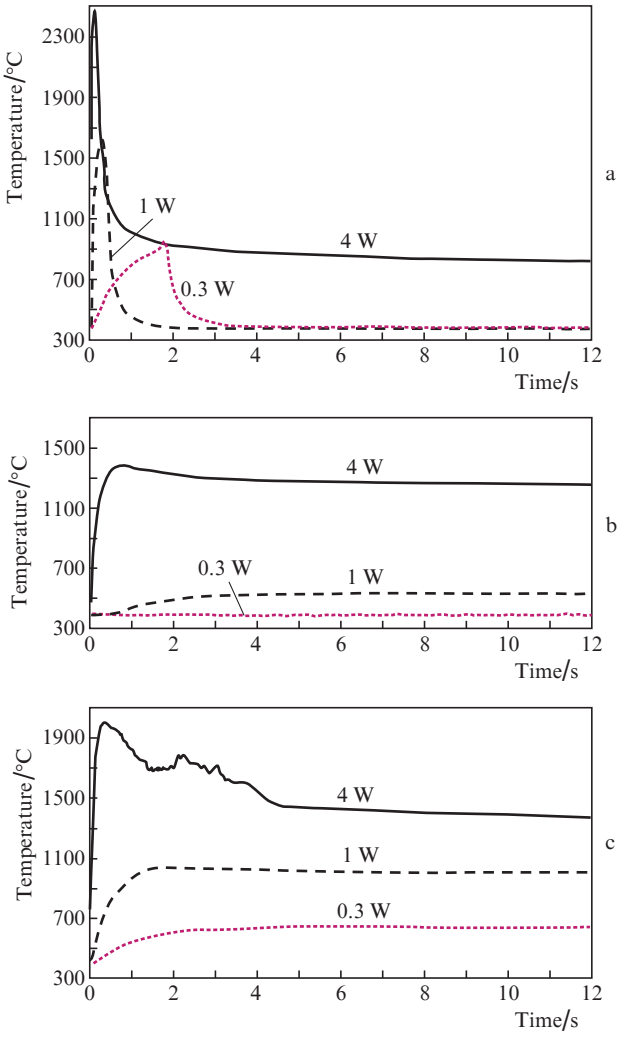

Figure 5. Heating dynamics of the (a) thin-film, (b) planar 3D and (c) spherical 3D COTFCs at different average powers of the 980-nm semiconductor laser beam incident on the converters.

for all the converters and the same method for evaluating heating efficiency (at the instant of failure).

The thin-film converter was destroyed at all average laser output powers: the carbon film was removed and, at a constant laser output power, the surface temperature of the converter began to decrease. Among the converters studied here, this one showed the highest surface heating efficiency, 3000 °C W^{-1}, at an incident laser radiation power of 0.3 W at the instant of converter failure (after 1.8 s of exposure), which was probably due to the small thickness and large absorption coefficient of the carbon film (22 cm^{-1} [40]) and the poor thermal contact between the film and fibre. Visual inspection of the converter after the exposure to laser light showed that there was no film on its surface, i.e. the carbon film was destroyed. Clearly, after the film was destroyed there was no absorber and the converter stopped being heated.

The maximum temperature, after reaching which the temperature of the converter begins to decrease, depends on the average incident laser beam power. At incident powers of 0.3 and 1 W, damage of the film after exposure to laser light for 10 s was followed by cooling of the converter to a temperature corresponding to the sensitivity limit of the Alta-ST system (390 °C), whereas at an average power of 4 W the converter cooled to a temperature of 800 °C over a period of 10 s. The converter surface heating efficiency was then about 200 °C W^{-1}. The data in Fig. 5a demonstrates that, in this case, the thin-film converter was heated to temperatures above 2000 °C. As shown earlier [29], such temperatures lead to the formation of nanoparticles of amorphous carbon, which probably deposits on the walls of microbubbles resulting from quartz glass melting (boiling) in the near-surface region of the distal fibre end. Thus, after disintegration of the film, the optical fibre surface is covered with a layer containing microbubbles whose inner surface is coated with amorphous carbon. Absorbing laser light, they heat the converter. Figure 2c shows a photograph of the thin-film converter after exposure to laser light with an average power of 4 W. It is seen that the surface of the converter is covered with a layer of microbubbles, with no carbon film.

The temperature of the planar 3D converter at an average laser output power of 0.3 W did not exceed the sensitivity limit of the measuring system. At an average power of 1 W, the efficiency of the laser heating of the converter surface after exposure to laser light for 10 s was about 550 °C W^{-1}, and the appearance of the converter remained unchanged. At an average power of 4 W, the heating efficiency after exposure to laser light for 10 s was about 320 °C W^{-1}, the temperature of the converter exceeded 1200 °C, and its surface had no carbon film. The disappearance of the carbon film on the surface of the converter can be accounted for by carbon combustion in air at temperatures above 800 °C [43]. Figure 3c shows a photograph of the planar 3D converter after laser exposure at an average power of 4 W. It is seen that the surface of the converter is covered with a layer of microbubbles, with no carbon film.

In the case of the spherical 3D converter, the efficiency of the laser heating of the converter surface after exposure to laser light with an average power of 0.3 W for 10 s was about 2100 °C W^{-1}, and the appearance of the converter after the exposure remained unchanged. At an average power of 1 W, the heating efficiency after exposure to laser light for 10 s was about 1000 °C W^{-1} and the surface of the converter had no carbon film. At an average power of 4 W, the efficiency of the laser heating of the converter surface after exposure for 10 s decreased to 350 °C W^{-1}, the temperature of the converter reached 2000 °C, and its surface had no carbon film.

The drop in heating efficiency can be accounted for by quartz glass melting in the modified layer (containing microbubbles), which leads to changes in microbubble size and carbon concentration and the associated changes in absorption index. Figure 4c shows a photograph of the spherical 3D converter after exposure to laser light at an average power of 4 W. It is seen that the surface of the converter is covered with a melted layer of microbubbles, with no carbon film.

4. Theoretical study of the heating dynamics of the COTFCs

In modelling each of the converters, we relied on optical microscopy data on the characteristic size and structure of the COTFCs. Since the absorption coefficient of quartz glass at the wavelength of the laser used in this study is extremely small [42], the COTFCs can only be heated through light absorption in the carbon film. The film may consist of amorphous carbon, whose absorption coefficient at a wavelength of 980 nm is about 22 cm^{-1} [29, 40]. The film may be located on both the outer surface of the COTFCs and the inner surface of the microbubbles in the bulk of the quartz glass. Based on the optical microscopy data on the geometry of the samples used in this study, the film thickness in our simulations of the thin-film converter was taken to be 50 μm on its end face and 30 μm on its lateral surface. In the case of the 3D converters, the film thickness was taken to be 5 μm on the surface of the COTFCs and 1 μm on the microbubbles surface [41]. The structural models of the converters and the model for the structure of the COTFC material are schematised in Fig. 6.

According to previous findings [41], the absorption coefficient of the material of the converter containing microbubbles is 2.1 mm^{-1}, and the modified layer of the COTFC consists of 45.7% quartz glass, 45.7% air and 8.6% carbon.

In our optical simulations, we used TracePro 6.0 software (Lambda Research Corporation, USA). For each converter, we constructed a 3D model that took into account its dimensions. We modelled processes in a fibre with a core diameter of 400 μm. The outer carbon film on both the thin-film and 3D converters was uniform and isotropic, and the absorption coefficient and refractive index of its material (amorphous carbon) were 22 mm^{-1} and 1.57, respectively [40]. The layer of microbubbles in the 3D COTFCs was also uniform and isotropic, but its absorption coefficient and refractive index were 2.1 mm^{-1} and 1.27, respectively [41]. It was covered with an isotropic film identical in optical characteristics to the outer carbon film of the thin-film converter. The dimensions of the converters in our simulations are indicated in Fig. 6.

Using ray tracing, we evaluated the fraction of laser light absorbed in the COTFCs and the absorbed laser power distribution in the bulk of the converters. The heat source distribution (Fig. 7) was obtained under the assumption that all the absorbed laser energy was converted into heat. It is seen that the heat sources are concentrated in the outer carbon film in the thin-film converter and in the layer containing microbubbles in the planar 3D converter, whereas those in the spherical 3D converter are distributed between the carbon film and the layer containing microbubbles. In all the converters, most energy is absorbed in a region near the fibre–converter interface.

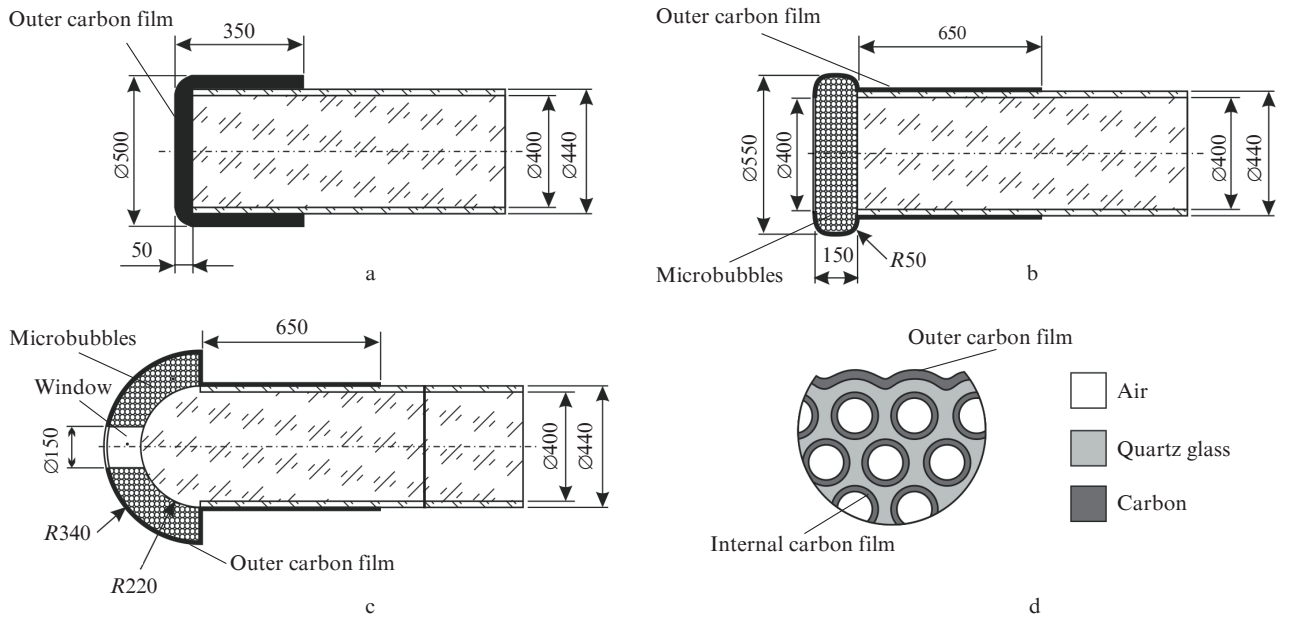

Figure 6. Structural models of the (a) thin-film, (b) planar 3D and (c) spherical 3D COTFCs and (d) model for the structure of the modified layer of the COTFCs. The dimensions are expressed in microns.

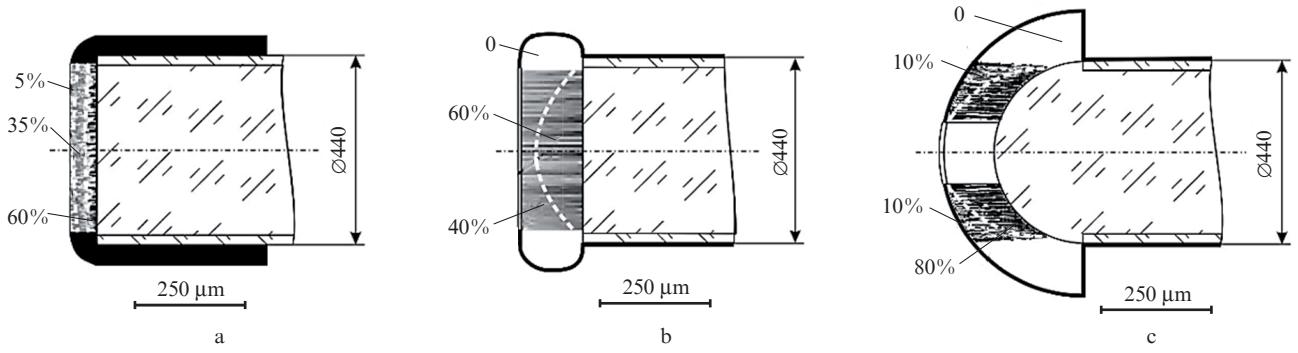

Figure 7. Heat source distribution in the bulk of the (a) thin-film, (b) planar 3D and (c) spherical 3D converters. The percentages specify the fraction of absorbed energy in a particular region of the converter. The dimensions are expressed in microns.

In our thermophysical simulations, we used COMSOL Multiphysics 4.3 software (COMSOL Inc., USA). The geometric model of the COTFCs was identical to that used in our optical simulations. The outer carbon film in the thin-film and 3D converters was uniform and isotropic, and its material (amorphous carbon) had a density of 1700 kg m^{-3}, specific heat of 690 J kg^{-1} K^{-1} and thermal conductivity of 375 W m^{-1} K^{-1} [43]. The 3D COTFCs were uniform and isotropic, but had a density of 1125 kg m^{-3}, specific heat of 850 J kg^{-1} K^{-1} and thermal conductivity of 1 W m^{-1} K^{-1} [41]. The solution was subject to the boundary condition that the temperature be constant (+20 °C) at the input fibre end. The length of the optical fibre was 3000 mm. Convection and radiation heat exchange processes took place on all the outer surfaces of the COTFCs (convection heat exchange coefficient, 1 W m^{-2} K^{-1}; emissivity factor, 0.92). The COTFCs contained 3D heat sources. Using the simulations, we assessed the steady-state temperature reached by the COTFCs at a given absorbed laser power and the heating dynamics of the COTFCs at a fixed average laser output power.

Taking into account the high repetition rate of the laser pulses (2 kHz), their short duration (400 μs) and the considerable time interval between measurements (30 ms), we conclude that the measured temperature in this study corresponds to the converter temperature averaged over the time of 60 laser pulses. Because of this, the contribution of an individual pulse cannot be detected in experiments, so the repetitive laser pulse generation can be left out of consideration in simulations and the laser output can be thought of as continuous, with an average power corresponding to that in our experiments.

The structural model of the OTFCs allowed us to take into account the contribution of outer carbon film disintegration to the heating dynamics of the converters. Heating the film to a temperature of 800 °C initiates the combustion of the carbon in the film as a result of reaction with the oxygen present in air around the COTFC [44]. Since oxygen inflow can be thought of as infinite, all the carbon on the surface of the COTFC will burn down after a certain length of time. The outer carbon film is a thin shell, which means that its thickness can be neglected in thermophysical simulation and the

film can be thought of as a surface heat source. We believe that, if the incident laser beam power and the properties of the film do not vary, the fraction of radiation absorbed in the film depends only on its thickness.

When the temperature reaches 800 °C and the film is heated further, it burns off and its thickness decreases. Therefore, in simulating this process, film burn-off can be represented as a gradual reduction in the power of the surface heat source. The simulation procedure and results for the contribution of outer carbon film disintegration to the heating dynamics of the converters were described previously [41]. When the outer carbon film is heated by laser radiation, the resulting deformation may change the thermal contact between the film and the surface of the quartz glass fibre, which should also be taken into account in simulation.

A different situation occurs in the case of the carbon present inside microbubbles. This carbon can react with only a limited volume of oxygen in each microbubble. With allowance for the geometry of the model described above, calculation of the weight fractions of oxygen and carbon suggests that the amount of oxygen in the microcavities is only sufficient for the combustion of less than 1% of the carbon present on the walls of the microcavities. Thus, most of the carbon present in the microbubbles does not participate in chemical reactions and, hence, its absorptive power remains unchanged up to temperatures corresponding to the melting point of quartz glass [42]. The melting of the quartz glass around the microbubbles leads to uncontrolled changes in the optophysical properties of the material of the COTFC, and the model can no longer adequately describe experimental data.

In this study, we simulated the temperature distribution in the converters, including the underlying fibre. The temperature profile along the length of the converters was found to be nonuniform. In particular, at an incident beam power of 0.3 W, the simulated temperature after 1 s of exposure is 780 °C on the surface of the thin-film converter (800 ± 50 °C in our experiments) and just 480 °C at a distance of 0.5 mm from its end. In the case of the planar 3D converter, the temperature after exposure for 10 s is 550 °C on the converter surface (550 ± 50 °C in our experiments) and 450 °C at a distance of 0.5 mm from its end. In the case of the spherical 3D converter, the temperature after 10 s reaches 1050 °C on its surface (1000 ± 50 °C in our experiments) and 800 °C at a distance of 0.5 mm from its end.

Figures 8–10 present experimentally determined temperature fields on the surface of the thin-film and 3D converters exposed to 980-nm semiconductor laser radiation and the corresponding simulation results in the above model, and illustrate the surface heating dynamics of the converters.

It is worth noting that the simulated temperature on the COTFC surface correlates well with the experimentally measured temperature, which confirms that the models used in this study for the COTFCs work well for real converters.

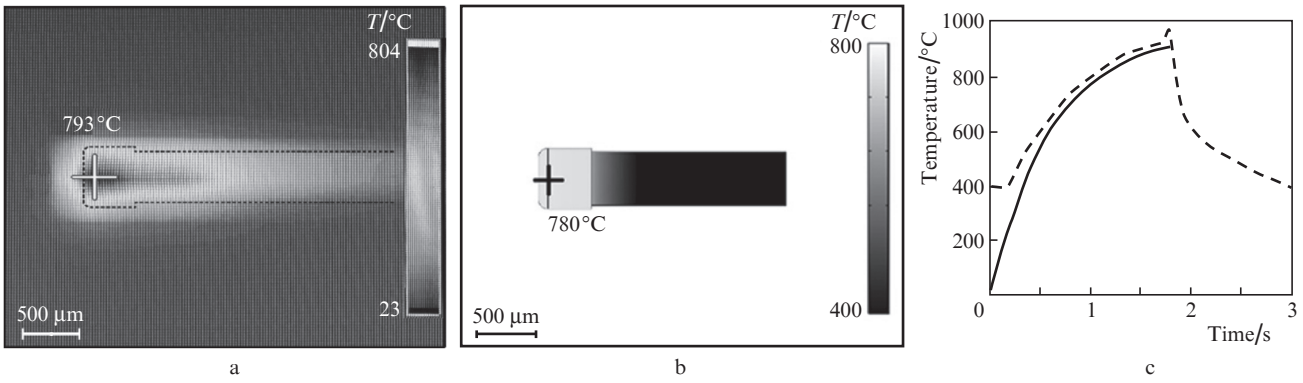

Figure 8. (a) Experimentally determined and (b) simulated temperature field on the surface of the thin-film COTFC after exposure to laser light for 1 s; (c) experimentally determined (dashed line) and simulated (solid line) heating dynamics on the converter surface at the point marked by a cross (average power, 0.3 W; wavelength, 980 nm).

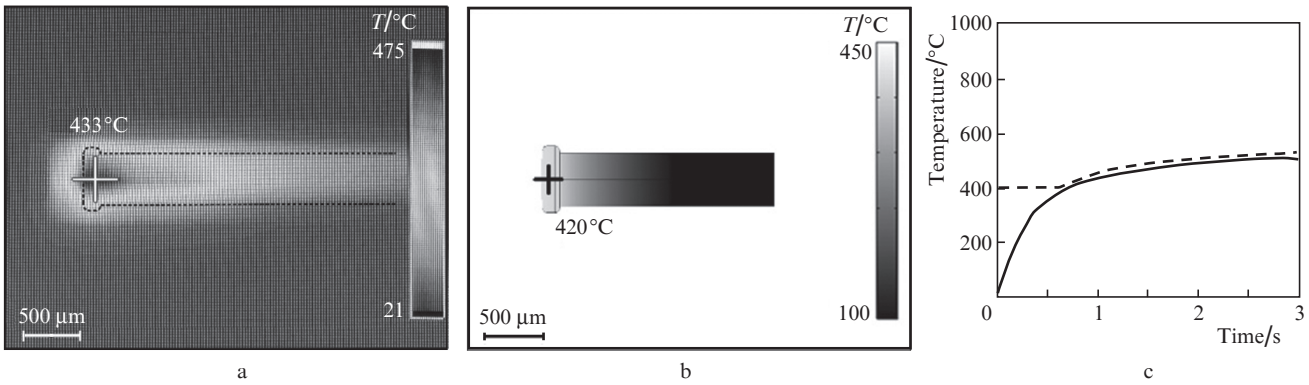

Figure 9. Same as in Fig. 8 but for the planar 3D COTFC at an average power of 1 W.

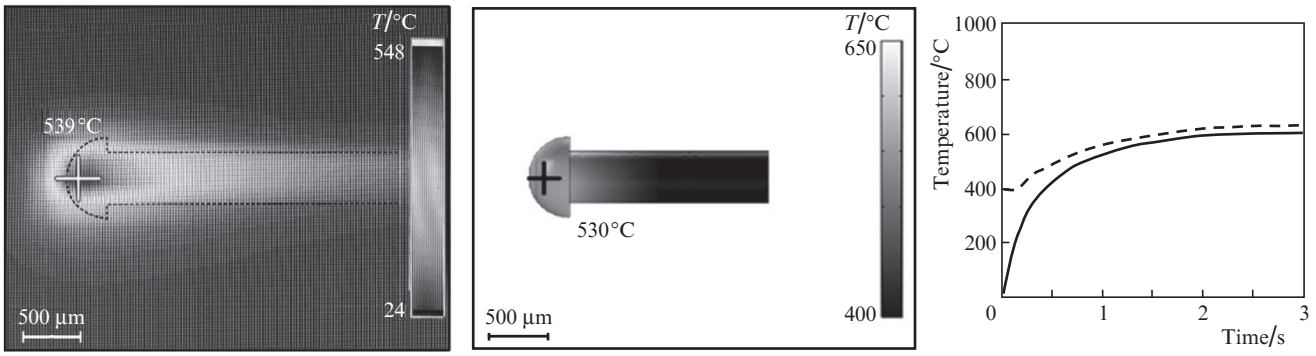

Figure 10. Same as in Fig. 8 but for the spherical 3D COTFC.

5. Conclusions

We have investigated the structure and heating dynamics of COTFCs for laser surgery. The efficiency of laser heating of the converter surface in air has been shown to depend on the type of converter and the average incident power. The efficiency varies with time, which is caused by the disintegration of the absorbing structures of the converter (carbon film and microbubbles) and the melting of the quartz glass fibre in contact with them. The highest heating efficiency was offered by the thin-film converter: 3000 °C W^{-1}. This type of converter was destroyed after a few seconds of exposure to laser radiation, even at an average power of 0.3 W. The lowest surface heating efficiency was observed in the case of the planar 3D converter: 550 °C W^{-1}. This type of converter remained intact at an average power of 1 W, whereas exposure to laser radiation with an average power of 4 W removed the carbon film and reduced the surface heating efficiency to a level of 320 °C W^{-1}, which then persisted until the end of the experiment.

We have constructed structural models of the converters. As the main structures absorbing laser radiation in the converters, we considered the carbon film and microbubbles resulting from the melting of the quartz glass during the fabrication and service of the converters and having carbon on their surface. We performed optical and thermophysical simulations in the proposed models. The simulation results on the heating of the converters are in satisfactory agreement with experimental data.

References

1. Rai P.K. In, *Emerging Trends in Laser & Spectroscopy and Applications* (New Delhi: Allied Publishers, 2010) p. 140.
2. Gubitosi A., Ruggiero R., Ortolani R., Podzemny V., Parmeggiani D., Esposito E., Foroni F., Esposito A., Villaccio G. *Ann. Ital. Chir.*, **75**, 515 (2012).
3. Kaufmann R., Hartmann A., Hibst R. *J. Dermatol. Surg. Onc.*, **20**, 112 (1994).
4. Rao G., Tripthi P.S., Srinivasan K. *Int. J. Laser Dent.*, **2**, 74 (2012).
5. Kaufmann R., Hibst R. *Clin. Exp. Dermatol.*, **15**, 389 (1990).
6. Wieliczka D.M., Weng S., Querry M.R. *Appl. Opt.*, **28**, 1714 (1989).
7. Romanos G., Nentwig G.H. *J. Clin. Laser Med. Sur.*, **17**, 193 (1999).
8. Sanz-Moliner J.D., Nart J., Cohen R.E., Ciancio S.G. *J. Periodontol.*, **84**, 152 (2013).
9. Qafmolla A., Bardhoshi M., Gutknecht N., Bardhoshi E. *ESJ*, **10**, 334 (2014).
10. Angermair J., Dettmar P., Linsenmann R., Nolte D.J. *Cosmet. Laser Ther.*, **17**, 296 (2015).
11. Shtirshnaider Yu.U., Volnukhin V.A. *Vestn. Dermatol. Venerol.*, **6**, 98 (2009).
12. Romanos G.E., Belikov A.V., Skrypnik A.V., Feldchtein F.I., Smirnov M.Z., Altshuler G.B. *Laser. Surg. Med.*, **47**, 411 (2015).
13. Vogel A., Venugopalan V. *Chem. Rev.*, **103**, 577 (2003).
14. Altshuler G.B., Belikov A.V., Skrypnik A.V., Fel'dshtein F.I. *Innovatsionnaya Stomatol.*, **1**, 2 (2012).
15. Bashkatov A.N., Genina E.A., Kochubey V.I., Tuchin V.V. *J. Phys. D: Appl. Phys.*, **38**, 2543 (2005).
16. Bashkatov A.N., Genina E.A., Tuchin V.V. *J. Innovative Opt. Health Sci.*, **4**, 9 (2011).
17. Beer F., Körpert W., Passow H., Steidler A., Meinl A., Buchmair A.G., Moritz A. *Laser. Med. Sci.*, **27**, 917 (2012).
18. Capon A., Mordon S. *Am. J. Clin. Dermatol.*, **4**, 1 (2003).
19. Rizzo L.B., Ritchey J.W., Higbee R.G., Bartels K.E., Lucroy M.D. *J. Am. Vet. Med. Assoc.*, **225**, 1562 (2004).
20. Skrypnik A.V. *Izv. Vyssh. Uchebn. Zaved., Priborostr.*, **56**, 37 (2013).
21. Belikov A.V., Feldchtein F.I., Altshuler G.B. US Patent № 2012/0123399 A1/№ 13/379,916; appl. 31.12.2010; pub. 17.05.2012.
22. Altshuler G.B. *Proc. 19th Annual Conf. of the Academy of Laser Dentistry* (Scottsdale, AZ, USA, 2012).
23. Dental Photonics, Inc. *Alta-ST Soft Tissue Surgical Modular System User Manual* (Walpole, MA, USA, 2015).
24. Belikov A.V., Skrypnik A.V., Shatilova K.V. *Front. Optoelectron.*, **8**, 212 (2015).
25. Yusupov V.I., Chudnovskii V.M., Bagratashvili V.N. *Laser Phys.*, **20**, 1641 (2010).
26. Yusupov V.I., Chudnovskii V.M., Bagratashvili V.N. *Laser Phys.*, **21**, 1230 (2011).
27. Bagratashvili V.N., Yusupov V.I., Chudnovskii V.M. *Proc. III Int. Symp. 'Topical Problems of Biophotonics'* (St. Petersburg–N. Novgorod, 2011) p. 269.
28. Yusupov V.I., Chudnovskii V.M., Bagratashvili V.N. In: *Hydrodynamics–Advanced Topics* (Rijeka, Croatia: InTech, 2011)
29. Belikov A.V., Skrypnik A.V., Zulina N.A. *Izv. Vyssh. Uchebn. Zaved., Priborostr.*, **56**, 50 (2013).
30. Abela G.S., Fenech A., Crea F., Conti C.R. *Laser. Surg. Med.*, **5**, 327 (1985).
31. Amin Z. *Laser. Med. Sci.*, **10**, 157 (1995).
32. Van den Bos R.R., Kockaert M.A., Neumann H.M., Bremmer R.H., Nijsten T., van Gemert M.J. *Laser. Med. Sci.*, **24**, 247 (2009).
33. O'Reilly G.V. US Patent № 4735201/4,735,201; appl. 30.01.1987; pub. 13.08.1987.
34. Friedman J. US Patent № 3875945/3,875,945; appl. 02.11.1973; pub. 08.04.1975.
35. Sivriver A., Boutoussov D. US Patent № 20150230865; appl. 20.02.2015; pub. 27.08.2015.
36. Skrypnik A.V. *Izv. Vyssh. Uchebn. Zaved., Priborostr.*, **5**, 385 (2015).

37. Welch A.J., Bradley A.B., Torres J.H., Motamedi M., Ghidoni J.J., Pearce J.A., Hussein H., O'Rourke R.A. *Circulation*, **76** (5), 1353 (1987).
38. Doshi Y., Shah M., Khandge N., Sanghavi A.J. *Oral Laser Appl.*, **10**, 165 (2010).
39. Biolase Technology, Inc. *Ezlase User Manual* (Irvine, CA, USA, 2015).
40. Mahtani P. *Doct. diss.* (University of Toronto, Toronto, 2010).
41. Belikov A.V., Skrypnik A.V., Kurnyshev V.Y. *Proc. SPIE Int. Soc. Opt. Eng*., **9917**, 99170G (2016).
42. Postnikov V.S. *Opticheskoe materialovedenie: kurs lektsii* (Optical Materials Research: A Set of Lectures) (Perm: Permsk. Nats. Issled. Politekh. Univ., 2013).
43. Sheludyak Yu.E., Kashporov L.Ya., Malinin L.A., Tsalkov V.N. *Teplofizicheskie svoistva komponentov goryuchikh sistem* (Thermophysical Properties of Components of Combustible Systems) (Moscow: NPO Infor TEI, 1992) p. 184.
44. Predvoditelev A.S., Khitrin L.N., Tsukhanova O.A., Kolodtsev Kh.I., Grozdovskii M.K. *Gorenie ugleroda* (Carbon combustion) (Moscow: Akad. Nauk SSSR, 1949).